

# An Interpretable Neural Network for Configuring Programmable Wireless Environments

Christos Liaskos\*, Ageliki Tsioliariidou\*, Shuai Nie<sup>‡</sup>, Andreas Pitsillides<sup>†</sup>, Sotiris Ioannidis\*, and Ian Akyildiz<sup>†‡</sup>

\*Foundation for Research and Technology - Hellas (FORTH), emails: {cliaskos,atsiolia,sotiris}@ics.forth.gr

<sup>†</sup>University of Cyprus, Computer Science Department, email: Andreas.Pitsillides@ucy.ac.cy

<sup>‡</sup>Georgia Institute of Technology, School of Electrical and Computer Engineering, emails: {shuainie,ian}@ece.gatech.edu

**Abstract**—Software-defined metasurfaces (SDMs) comprise a dense topology of basic elements called meta-atoms, exerting the highest degree of control over surface currents among intelligent panel technologies. As such, they can transform impinging electromagnetic (EM) waves in complex ways, modifying their direction, power, frequency spectrum, polarity and phase. A well-defined software interface allows for applying such functionalities to waves and inter-networking SDMs, while abstracting the underlying physics. A network of SDMs deployed over objects within an area, such as a floorplan walls, creates programmable wireless environments (PWEs) with fully customizable propagation of waves within them. This work studies the use of machine learning for configuring such environments to the benefit of users within. The methodology consists of modeling wireless propagation as a custom, interpretable, back-propagating neural network, with SDM elements as nodes and their cross-interactions as links. Following a training period the network learns the propagation basics of SDMs and configures them to facilitate the communication of users within their vicinity.

**Index Terms**—Wireless, Propagation, Software control, Metasurfaces, Neural Network, Interpretable.

## I. INTRODUCTION

With the proliferation of smart wireless devices and burgeons of the Internet of Things (IoT) over recent years, wireless communication systems have experienced unprecedented demands for higher data rates, smaller latency, better services, and lower prices. These requirements have driven the research efforts into the fifth-generation wireless networks, narrow-band IoT, among other promising techniques to tackle the open problems of limited spectrum resources and high user densities [1]. Most of the proposed solutions focus on the improvement of transceivers, for example, the massive MIMO technique and millimeter wave solutions. However, a largely overlooked factor that directly influences the performance of the wireless system is the propagation environments. With the use of novel materials, the propagation environments can be turned into *programmable* media, yielding unparalleled, wired-level gains in wireless power transfer, and the mitigation of interference, Doppler effects and malicious eavesdropping [2].

In regular wireless propagation environments, EM waves undergo various interactions including reflections, diffractions, and scattering. Rich multi-path conditions are generated as a result of these interactions which, if not well-controlled, could destructively influence the users' communication. In order to exert deterministic, adaptive control over the wireless propagation phenomenon, a novel solution based on artificial

planar materials has been conceived, which utilizes software-defined metasurfaces (SDMs) [3]. SDMs sense and apply transformative control over EM waves impinging upon them, re-engineering their direction, polarization and phase, performing arbitrary wavefront shaping which indicatively includes focus, collimation and absorption (Fig. 1-left). SDM *tiles* are rectangular, connected SDM units that bear an IoT gateway, allowing a central computer to get or set their desired EM functionality. Such materials have also been recently generalized under the term *intelligent surfaces* [4]–[7], to denote their end-facility while abstracting the underlying physical-layer technology specifics.

Programmable wireless environments (PWEs) are created by coating major parts of a setting (e.g., ceilings in a floorplan [8]) with SDM tiles [2], [9], as shown in Fig. 1-right. A central computer senses the EM profile and connectivity objectives of users present in the environment, and adaptively *configures* the matching functionality for each SDM tile [10].

In this paper, we propose an approach based on machine learning algorithms, in particular, neural networks, to adaptively configure PWEs for a set of users. The key-idea is that, since SDM tiles can regulate the distribution of power within a space, they can be represented by nodes in a neural network, while the power distribution can be mapped to neural network links and their weights. The weights are optimized via custom feed-forward/back-propagation processes, and are interpreted into SDM tile functionalities. The machine learning approach is shown to be intuitive in its representation and economic in its user of SDM tiles, compared to related approaches [10].

The remainder of this paper is organized as follows. Section II provides background information on the principles of SDMs and neural networks. Section III details the proposed neural net approach for configuring PWEs. Evaluation via ray-tracing follows in Section IV, along with a discussion of future directions. The paper is concluded in Section V

## II. BACKGROUND

*The structure of SDMs:* A metasurface is an engineered structure which is the two-dimensional representation of metamaterials with the basic element called “meta-atom”. In usual compositions, the substrate is dielectric and the meta-atom is conductive, which can be made of copper over silicon. Alternative conductors can be silver, gold, or graphene for operating frequencies in the terahertz band [11], [12]. Metasurfaces can

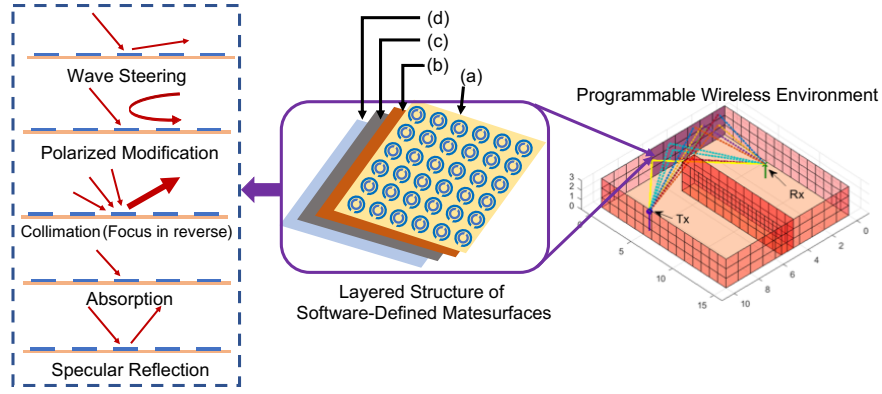


Fig. 1. Illustration of the SDM tile structure and its indicative EM functionalities (left), and the enabling operation mode in a PWE with a pair of transmitter and receiver (right). The layers of a SDM from top to bottom include (a) the metasurface plane, (b) the sensing and actuation plane, (c) the computing plane, and (d) the communications plane.

be designed to support the propagation of highly confined surface plasmon polariton (SPP) waves at microwave, millimeter wave, and even higher frequencies and to control these EM waves impinging on them [13]. In general, metasurfaces comprise several hundreds of meta-atoms, which results into fine-grained control over the EM wave interactions. In particular, the size of each meta-atom is comparable to the minimum intended interaction wavelength,  $\lambda$ , with  $\frac{\lambda}{10} \rightarrow \frac{\lambda}{5}$  constituting a common choice. The thickness of the metasurfaces is in the sub-wavelength scale, ranging between  $\frac{\lambda}{10}$  and  $\frac{\lambda}{5}$  as well.

The layered structure to enable various operation modes of metasurfaces is given in Fig. 1. The meta-atoms can have different shapes, including the shown split-ring structure and more complicated ones [9]. The total EM response of the metasurface is then derived as the total emitted field by all surface currents, and can take completely engineered forms, achieving custom phase shift, polarization tuning, and so on. In fact, the meta-atoms can be viewed as either input or output antennas, connected in custom topologies via the switch elements. Impinging waves enter from the input antennas, get routed according to the switch element states, and exit via the output antennas, exemplary achieving customized reflection.

*Neural Network for PWEs:* Among many machine learning algorithms, neural networks are known for their high efficiency in finding optima to complex problems and making accurate predictions. A neural network consists of an input layer with input units, at least one layer of hidden nodes neurons, and an output layer with multiple output units [14]. The interconnected nodes and layers have associated weights and activation levels to the links, while each node has an input function, an activation function, and an output. For a PWE application of neural networks, the general concept can be described as follows. The input layer units are configured by the propagation environments including the numbers and locations of transmitters (TXs) and receivers (RXs), densities and dimensions of metasurface tiles, operating frequencies, noise levels, among others. The corresponding output links can be activated at certain levels. For example, if a metasurface tile

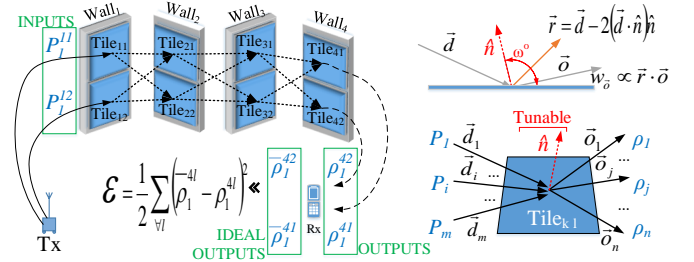


Fig. 2. Conceptual representation of wireless propagation as a neural network.

is in proximity to the TX and a non-line-of-sight RX which can be adjusted by its azimuth angle to reflect the impinging signal towards the RX, the activation function is related to the received signal strength indicator (RSSI) and the angle of arrival (AoA) of the signal.

In order for the neural network to generate a desired model, the process of determining weights to nodes in each layer is of critical importance. Among many options, backpropagation is the most widely employed method in weight optimization. The idea of backpropagation is to adjust the weights of nodes based on the errors at the output layer [15]. Since in the neural network each hidden node contributes to the resultant error of its connected output nodes, the error can be divided according to the strength of each connection between a hidden node and the output node, hence the resultant error is propagated back to each layer to adjust the weights which will eventually minimize the new error.

It is noted that the present work employs custom neural networks, going beyond their standard composure and conceptual operation. We proceed to detail the specifics of the proposed solution in the next Section.

### III. NNCONFIG: NEURAL NET-CONFIGURED PWEs

Consider a PWE environment comprising a wireless transmitter (Tx), a receiver (Rx) and a set of walls-scatterers coated

with SDM tiles. This environment is illustrated in Fig. 2.

We assume that EM waves transmitted from the Tx impinge upon the first wall. Thus, each SDM tile over wall<sub>1</sub> has its own “input” impinging power. Each tile can be tuned to split and redirect its impinging power to other walls and tiles at their line-of-sight (LOS). These LOS links are shown as dashed arrows in Fig 2. Finally, the Rx receives part of the originally transmitted power via tiles in his LOS. The received power from each Rx link can be considered as the “output” of the propagation process. The “ideal output” represents lossless propagation, i.e., receiving the total of the transmitted power. The distribution over the Rx links respects the corresponding receiving gains of the Rx device, as derived by the Rx antenna pattern and the active MIMO configuration. The ideal and received outputs can be compared, in order to obtain a metric of deviation,  $\mathcal{E}$ , as shown in Fig. 2.

We proceed to study the inputs/outputs of a single tile and their relation. Following the SDM model of [10], the SDM tile steering can be modeled as virtually rotating the tile surface normal unit vector  $\hat{n}$ . The steering effect is shown in the top-right inset of Fig. 2. The reflected wave direction,  $\vec{r}(\hat{n}, \vec{d}) = \vec{d} - 2(\vec{d} \cdot \hat{n})\hat{n}$  [16], for a wave impinging from a direction  $\vec{d}$  can be altered by tuning  $\hat{n}$ , which is achieved by setting the SDM active elements accordingly. This information is provided by the SDM manufacturer, e.g., in the form of a lookup table.

A reflection  $\vec{r}(\hat{n}, \vec{d})$  may not coincide exactly with a given inter-tile, “outgoing” link direction  $\vec{o}$ . Thus, we proceed to make a *heuristic* assumption that the power fraction,  $w_{\vec{o}}$ , over an “outgoing” link  $\vec{o}$  is:

$$w_{\vec{o}}(\hat{n}, \vec{d}) = \frac{\max\{\vec{r}(\hat{n}, \vec{d}) \cdot \vec{o}, 0\}}{\sum_{\forall \vec{o}} w_{\vec{o}}}, \quad (1)$$

i.e., the projection of  $\vec{r}$  over  $\vec{o}$  normalized across all outgoing links, assuming that  $\vec{o}$  and  $\vec{d}$  are unit vectors. A negative inner product in relation (1) implies that vectors  $\vec{r}$ ,  $\vec{o}$  do not face in the same direction and, thus,  $w_{\vec{o}}$  should intuitively be zero.

Based on these remarks, we proceed to model the wireless propagation as a neural network with walls as layers and tiles as nodes, and define feed-forward and back-propagate processes as follows:

1) *Feed-forward*: Consider the general case of tile <sub>$k,l$</sub> , indexed and denoted as shown in Fig. 2. The power at each of its outgoing links is:

$$\rho_j^{(k,l)} = \sum_{\forall \vec{d}_i} w_{\vec{d}_i}(\hat{n}, \vec{d}_i) \cdot P_i^{(k,l)}, \quad (2)$$

which serves as input power for the next wall-layer, since SDMs can employ collimation functionalities to focus their total outgoing power to the next tile [10]. At the final wall-layer,  $k = \kappa$ , the metric of deviation,  $\mathcal{E}$ , is calculated as:

$$\mathcal{E} = \frac{1}{2} \sum_{\forall l} \left( \bar{\rho}_1^{(\kappa,l)} - \rho_1^{(\kappa,l)} \right)^2 = \frac{1}{2} \sum_{\forall l} \delta_l^2, \quad (3)$$

where  $\bar{\rho}$  denotes ideal output power ratio, and  $\delta_l = \bar{\rho}_1^{(\kappa,l)} - \rho_1^{(\kappa,l)}$ .

2) *Back-propagation*: Once the walls-layers have been iterated over until the final layer, each tile-node at each wall-layer (in reverse order) deduces the effect of its currently active  $\hat{n}$  vector to the deviation  $\mathcal{E}$ , and updates  $\hat{n}$  to a new value  $\hat{n}_*$ . For simplicity we will focus on the 2D case where  $\hat{n}$  is defined by a single angle  $\omega$ , as shown in Fig. 2 (top-right). The corresponding update rule from  $\omega$  to  $\omega_*$  at tile  $(k,l)$  follows the generalized delta rule [17]:

$$\omega_*^{(k,l)} = \omega^{(k,l)} - \eta \cdot \left( \frac{\partial \mathcal{E}}{\partial \omega} \right)^{(k,l)} \cdot \mathcal{S}^{(k,l)}, \quad (4)$$

where  $\eta \in (0, 1]$  is the network’s learning rate, and  $\mathcal{S}^{(k,l)}$  is a factor denoting the significance of tile  $(k,l)$  with regard to the propagation. For the final wall-layer  $k = \kappa$  we define that  $\mathcal{S}^{(\kappa,l)} = \delta_l$  (i.e., its deviation from the local ideal output). For  $k \neq \kappa$  we define it as the total power impinging on the tile, i.e.,  $\mathcal{S}^{(\kappa,l)} = \sum_{\forall i} P_i^{(k,l)}$ .

Finally, we provide the following formulas for  $\left( \frac{\partial \mathcal{E}}{\partial \omega} \right)^{(k,l)}$  per indexed layer, omitting the proofs:

$$\begin{aligned} \left( \frac{\partial \mathcal{E}}{\partial \omega} \right)^{(\kappa,l)} &= \delta_l \cdot \frac{\partial \rho_1^{(\kappa,l)}}{\partial \omega^{(\kappa,l)}} \\ \left( \frac{\partial \mathcal{E}}{\partial \omega} \right)^{(\kappa-1,l)} &= \sum_{\forall j} \underbrace{\frac{\partial \rho_j^{(\kappa-1,l)}}{\partial \omega^{(\kappa-1,l)}}}_{e_j} \cdot \underbrace{\delta_j \cdot w_{\vec{o}_j^{(\kappa-1,l)}}}_{a_j} = \mathbf{e}^{(\kappa-1,l)} \cdot \mathbf{a}^{(\kappa-1,l)} \\ &\dots \\ \left( \frac{\partial \mathcal{E}}{\partial \omega} \right)^{(k,l)} &= \sum_{\forall j} \frac{\partial \rho_j^{(k,l)}}{\partial \omega^{(k,l)}} w_{\vec{o}_j^{(k,l)}} (\mathbf{1} \cdot \mathbf{a}^{(j,l+1)}), \end{aligned} \quad (5)$$

where  $\mathbf{e}$  and  $\mathbf{a}$  are helping vectors defined as shown above, and  $\mathbf{1}$  is an all-ones vector with size equal to  $\mathbf{a}$ .  $\mathbf{e}$  is only used for facilitating the definition of  $\mathbf{a}$  in relation (5) and has not further use, while  $\mathbf{a}$  is updated recursively at each node. Its elements are the link weight products, for all paths leading from a right-layer neighbor to any output layer node.

The described feed-forward/back-propagate cycles can be executed in an online or offline manner, until the deviation  $\mathcal{E}$  stabilizes, reaches an acceptable level or an allocated computational time window expires. At this point, the PWE controller simply deploys EM functionalities at each tile  $(k,l)$ , matching the attained  $\omega^{(k,l)}$  (and, thus  $\hat{n}^{(k,l)}$ ) values. This trait makes the proposed approach a directly interpretable neural network configurator for PWEs. We denote this proposed approach as NNCONFIG and proceed to evaluate it via full PWE simulations.

#### IV. EVALUATION

We evaluate the performance of NNCONFIG in the PWE simulator presented in [10]. We seek to evaluate the potential of the proposed scheme in a ray-tracing setting, comparing its outcomes to: i) regular propagation, and ii) the KPCONFIG scheme for PWEs presented in [10].

KPCONFIG is novel scheme for configuring PWEs, which is based on the ray-routing principle [10]. The multiple rays that

TABLE I  
FLOORPLAN, USER LOCATION AND BEAM ORIENTATION COORDINATE SYSTEM. THE ORIGIN IS AT THE LOWER LEFT CORNER OF THE FLOORPLAN.

USER: POSITION, $\alpha, \phi, \theta$
0: [2.5, 7.5, 0.5], $40^\circ, 0^\circ, 0^\circ$
1: [7.5, 7.5, 0.5], $40^\circ, 0^\circ, 180^\circ$
COMM. PAIR: OBJECTIVE
0→1 : MAX. RECEIVED POWER

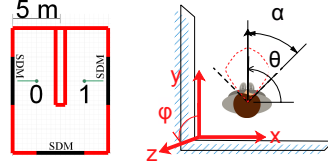


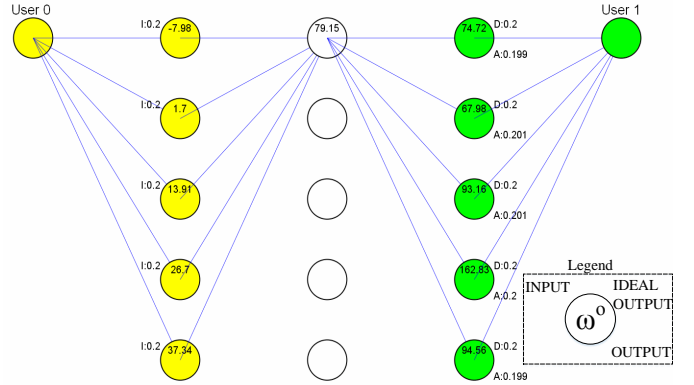
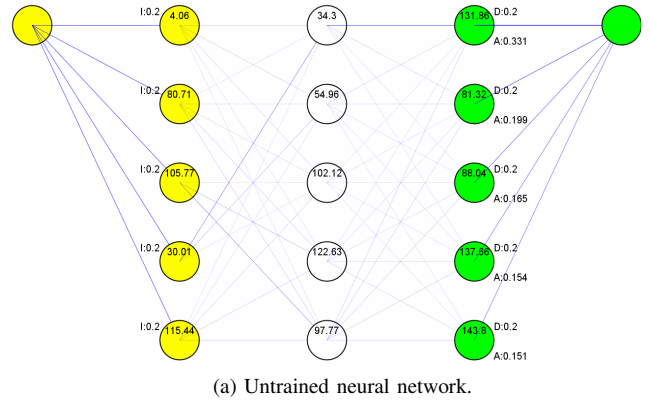
TABLE II  
SIMULATION PARAMETERS.

Ceiling Height	1 m
Tile Dimensions	1 × 1 m
Tile Functions	STEER, COLLIMATE, ABSORB
Non-SDM surfaces	Perfect absorbers (cf. red in Table I)
Frequency	2.4 GHz
Tx Power	-30 dBm
Antenna type	Single $a^\circ$ -lobe sinusoid, pointing at $\phi^\circ, \theta^\circ$ (cf. Table I)
Max ray bounces	5
Power loss per bounce	1 %

are emitted from a set of transmitters are minutely managed until their reception from the appropriate receivers, applying proper EM functions (steering, absorbing, collimating, polarizing, phase-modifying, etc.) to each tile. Its advantages include versatility in handling multiple users and multiple objectives, spanning QoS optimization, Doppler effect mitigation, wireless power transfer and security. One of the KPCONFIG principles is to use only one function per tile whenever possible. This implies the management of just one ray per tile, a principle that can allow for less complex and potentially more efficient EM functions, but also increases the number of active tiles.

We consider a Tx-Rx pair in the floorplan and setup shown in Table I. It comprises three walls that the Tx emissions must sequentially and necessarily hit to reach the Rx. We seek to tune each SDM tile in this setup so as to maximize the received power at the Rx. Table II summarizes the persistent simulator parameters across all subsequent tests. Note that the setup corresponds to 2D ray propagation in a 3D space (the tile size and floor height are equal), matching the relations (5) presented in Section III.

The NNCONFIG neural network representation of the simulation setup is shown in Fig. 3. The input to each tile of the first layer is the normalized portion of power impinging upon it via the links of user 0. Since the objective is to transfer all emitted power to user 1, these inputs can be *virtual* (i.e., not equal to the actual impinging power distribution). Thus, each input is set to 20 % of the total emitted power, for each of the five tiles in the first layer. Using the same principle, the ideal output is set to 20 % of the total power to reach the receiver. Since the inputs and outputs remain the same at every feed-forward/back-propagate cycle, a high learning rate is selected



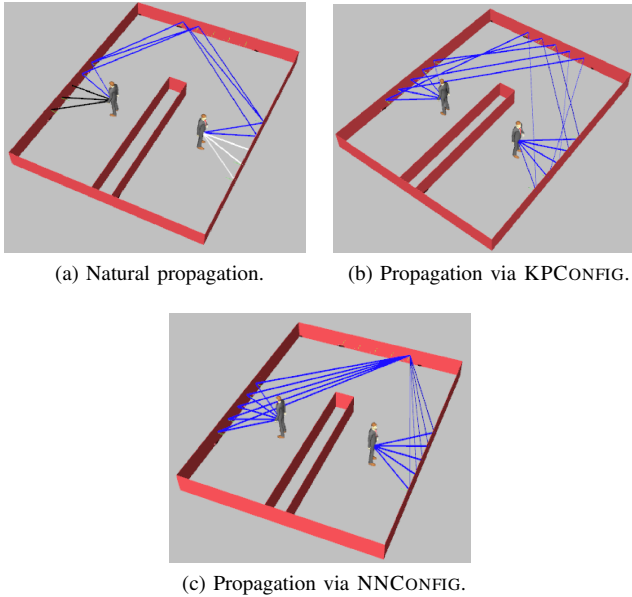
(b) Trained neural network after 2000 feed-forward/back-propagate cycles (learning rate  $\eta = 0.95$ , attained RMSE= $8 \cdot 10^{-4}$ ).

Fig. 3. The neural network corresponding to the studied setup and its untrained/trained states.

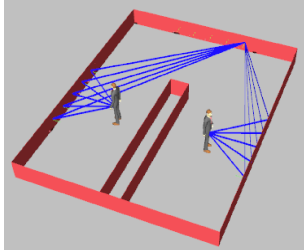
( $\eta = 0.95$ ). The initial  $\omega$  angle values per tile are randomized in the range  $[-90^\circ, 90^\circ]$ . This leads to the formation of the untrained network of Fig. 3a. Finally, the termination criterion is to reach a root mean square error (RMSE) of less than  $10^{-3}$ , which is achieved at approximately 2000 feed-forward/back-propagate cycles.

The trained network is shown in Fig. 3b. Notably, NNCONFIG finds a solution where only one tile is activated in the middle layer. This is the natural outcome of reinforcement learning around an “impactful” tile, i.e., one already managing a considerable part of the total impinging power. Thus, NNCONFIG is economic in terms of used tiles, which can be beneficial in terms of power expenditure and supported user capacity.

Visualizations of the ray-traced outcome per each compared scheme are given in Fig. 4. Regular propagation supports only symmetric (specular) ray reflection. As a result, it cannot steer  $\sim 60\%$  of the emitted power to the receiver; since 3 out of 5 rays (to the front and right of the transmitter) are directly reflected to absorbing areas. KPCONFIG works as intended and finds a solution that routes all power to the receiver. However, it uses all tiles in the middle wall, reaching full PWE capacity. NNCONFIG uses just one tile in the middle, in perfect match with the neural network abstraction in Fig. 3b.



(a) Natural propagation. (b) Propagation via KPCONFIG.



(c) Propagation via NNCONFIG.

Fig. 4. Wireless propagation visualized for each approach.

TABLE III  
RECEIVED POWER PER APPROACH.

Regular propagation	$-70.71 \text{ dBmW}$
KPCONFIG	$-49.87 \text{ dBmW}$
NNCONFIG	$-49.83 \text{ dBmW}$

The received power per scheme is given in Table III. All three propagation approaches are subject to receiving antenna aperture losses [10]. Regular propagation performs worse for two reasons. First, it loses  $\sim 60\%$  of the emitted power for the reasons described above. Second, it does not support collimation and focusing capabilities and is, thus, subject to the  $1/r^2$  power attenuation rule [10]. On the other hand, both KPCONFIG and NNCONFIG behave similarly in terms of received power, since they successfully groom and route all power from the transmitter to the receiver.

*Discussion and future work:* NNCONFIG exhibits potential for configuring PWEs in a tile-economic manner. It can minimize the number of tiles required for serving communication objectives. Moreover, it follows a representation of the PWE setting that is simple, intuitive and directly interpretable. Future work is directed towards extending the neural network representation to multiple users and multiple objectives. To this end, a promising direction is its combination with KPCONFIG in a hierarchical approach, where KPCONFIG coarsely routes EM waves at the level of wall orderings, and NNCONFIG deduces the exact EM functionality per tile.

## V. CONCLUSION

Programmable wireless environments allow for software-defined propagation of electromagnetic waves within a space, with tremendous potential for wireless communication. Special tiles made from planar, software-defined metamaterials receive programmatic commands and change their interaction with

impinging electromagnetic waves, benefiting wireless devices. The present paper introduced an interpretable neural network-based approach for configuring the behavior of tiles in such environments. Tiles and inter-tile power flow were mapped to neural network nodes and links respectively, and custom feed-forward and back-propagate processes were introduced. Evaluation via ray-tracing showed performance potential at the level of state-of-the-art solutions, with a distinct gain in reducing the total number of tiles required to be activated.

## ACKNOWLEDGMENT

This work was funded by the European Union via the Horizon 2020: Future Emerging Topics call (FETOPEN), grant EU736876, project VISORSURF (<http://www.visorsurf.eu>).

## REFERENCES

- [1] I. F. Akyildiz, S. Nie, S.-C. Lin, and M. Chandrasekaran, "5g roadmap: 10 key enabling technologies," *Computer Networks*, vol. 106, pp. 17–48, 2016.
- [2] C. Liaskos, S. Nie, A. Tsioliariidou, A. Pitsillides, S. Ioannidis, and I. Akyildiz, "A new wireless communication paradigm through software-controlled metasurfaces," *IEEE Communications Magazine*, vol. 56, no. 9, pp. 162–169, Sept 2018.
- [3] C. Liaskos, A. Tsioliariidou, A. Pitsillides, I. F. Akyildiz, N. V. Kantartzis, A. X. Lalas, X. Dimitropoulos, S. Ioannidis, M. Kafesaki, and C. Soukoulis, "Design and development of software defined metamaterials for nanonetworks," *IEEE Circuits and Systems Magazine*, vol. 15, no. 4, pp. 12–25, 2015.
- [4] C. Huang, G. Alexandropoulos, A. Zappone, M. Debbah, and C. Yuen, "Energy efficient multi-user MISO communication using low resolution large intelligent surfaces," in *IEEE GLOBECOM Workshops*. IEEE, 2018.
- [5] Q. Wu and R. Zhang, "Intelligent reflecting surface enhanced wireless network," *arXiv:1809.01423*, 2018.
- [6] —, "Beamforming optimization for intelligent reflecting surface with discrete phase shifts," in *ICASSP 2019*. IEEE, 2019, pp. 7830–7833.
- [7] S. Hu, F. Rusek, and O. Edfors, "Beyond massive mimo: The potential of data transmission with large intelligent surfaces," *IEEE Transactions on Signal Processing*, vol. 66, no. 10, pp. 2746–2758, 2018.
- [8] C. Liaskos *et al.*, "A novel communication paradigm for high capacity and security via programmable indoor wireless environments in next generation wireless systems," *Ad Hoc Networks*, vol. 87, pp. 1–16, 2019.
- [9] C. Liaskos, A. Tsioliariidou, A. Pitsillides, S. Ioannidis, and I. F. Akyildiz, "Using any surface to realize a new paradigm for wireless communications," *Commun. ACM*, vol. 61, no. 11, pp. 30–33, Oct. 2018. [Online]. Available: <http://doi.acm.org/10.1145/3192336>
- [10] C. Liaskos, A. Tsioliariidou, S. Nie, A. Pitsillides, S. Ioannidis, and I. Akyildiz, "Modeling, simulating and configuring programmable wireless environments for multi-user multi-objective networking," *arXiv preprint arXiv:1812.11429*, 2018.
- [11] A. Y. Zhu, A. I. Kuznetsov, B. Lukyanchuk, N. Engheta, and P. Genevet, "Traditional and emerging materials for optical metasurfaces," *Nanophotonics*, vol. 6, no. 2, pp. 452–471, 2017.
- [12] A. Fallahi and J. Perruisseau-Carrier, "Design of tunable biperiodic graphene metasurfaces," *Physical Review B*, vol. 86, no. 19, p. 195408, 2012.
- [13] M. J. Lockyear, A. P. Hibbins, and J. R. Sambles, "Microwave surface-plasmon-like modes on thin metamaterials," *Physical review letters*, vol. 102, no. 7, p. 073901, 2009.
- [14] V. Sze, Y.-H. Chen, T.-J. Yang, and J. Emer, "Efficient processing of deep neural networks: A tutorial and survey," *arXiv preprint arXiv:1703.09039*, 2017.
- [15] S. Dörner *et al.*, "Deep learning based communication over the air," *IEEE Journal of Selected Topics in Signal Processing*, vol. 12, no. 1, pp. 132–143, 2018.
- [16] E. Hitzer, "Introduction to clifford's geometric algebra," *arXiv preprint arXiv:1306.1660*, 2013.
- [17] K. Gurney, *An introduction to neural networks*. CRC press, 2014.